Metallography, Microstructure, and Analysis (2024) 13:332–338
https://doi.org/10.1007/s13632-024-01071-4

ORIGINAL RESEARCH ARTICLE

Effect of Initial ⟨0001⟩||RD Orientation on the Rolling Texture of AZ91 Alloy

Ebrahim Tolouie[1] · Roohollah Jamaati[1]

Received: 23 October 2023 / Revised: 26 February 2024 / Accepted: 21 March 2024 / Published online: 24 April 2024

Abstract
In the present research, for the first time, the ⟨0001⟩||RD as an initial texture for suppression of basal slip and the continuous β-$Mg_{17}Al_{12}$ phase for inhibition of extension twinning was used, simultaneously, to obtain non-basal orientation in the asymmetrically cold-rolled AZ91 magnesium alloy. The as-cast alloy consisted of α + β eutectic and α-Mg with two intermetallic phases ($Mg_{17}Al_{12}$ and Al_8Mn_5) which were located along grain boundaries and also inside the alpha grains. After 8 and 15% rolling reductions, the fraction of high-angle grain boundaries increased which was mainly due to the formation of many contraction and/or double twins. It was found that achieving non-basal texture in magnesium alloys during rolling deformation is possible. This was firstly due to the primary strong ⟨0001⟩||RD orientation, which was not favored for both prismatic and basal slips. Secondly, the incoherent β located at the boundaries of α grains suppressed the extension twin nucleation (which quickly strengthens basal texture) but did not inhibit the nucleation of double and contraction twins.

Keywords AZ91 magnesium alloy · Asymmetric cold rolling · Crystallographic texture · Microstructure

Introduction

Mg and its alloys are used in aircraft and automotive manufacturers due to the high strength-to-density ratio which leads to decreasing fuel consumption [1–3]. Despite its high specific strength, poor ductility at ambient temperature has significantly restricted the widespread use of Mg alloys in critical safety components [4]. The low ductility of Mg alloys is attributed to the low number of slip systems in the $\{0001\}$ of the hexagonal closed pack (HCP) crystal structure [5–7]. In addition, plastic deformation results in strong $\{0002\}$ basal texture [8–10]. This orientation leads to poor ductility at ambient temperature.

The poor ductility and anisotropic properties of magnesium can be modified by decreasing the intensity of $\{0002\}$ basal orientation [11–13]. Rare earth (RE) and Ca addition to Mg alloys, changing the strain path, and also the occurrence of recrystallization reduce the intensity of the basal orientation and lead to improving the formability and ductility [14–22]. However, achieving non-basal textures during the plastic deformation of Mg alloys was impossible [11–22].

During plastic deformation, the development of strong $\{0001\}$ texture firstly is owing to the prior activation of the $\{0001\}\left\langle 11\bar{2}0\right\rangle$ slip system. This slip system has the smallest critical resolved shear stress (CRSS) [8, 23, 24]. The formation of twins is associated with a rapid reorientation of the crystal [25–28]. $\left\{10\bar{1}2\right\}$ extension twins reorientate with $86°\left\langle 11\bar{2}0\right\rangle$ with respect to the parent grain, which can quickly stimulate the $\{0001\}$ slip activation and generation of intense basal orientation [29–32]. On the other hand, $\left\{10\bar{1}1\right\}-\left\{10\bar{1}2\right\}$ double twins and $\left\{10\bar{1}1\right\}$ contraction twins have an orientation relationship of $56°\left\langle 11\bar{2}0\right\rangle$ and $38°\left\langle 11\bar{2}0\right\rangle$ rotations between the untwined matrix and the twin variants [25, 28, 33]. Therefore, the contribution of double and contraction twins for the formation of $\{0002\}$ basal texture is low. However, according to the very low CRSS of extension twinning (2–2.8 MPa) [30, 34], activation of contraction twinning (with CRSS of 76–153 MPa) [30, 35] in Mg alloys is more difficult.

✉ Roohollah Jamaati
jamaati@nit.ac.ir

[1] Department of Materials Engineering, Babol Noshirvani University of Technology, Shariati Ave., Babol 47148–71167, Iran

According to the above, the extension twinning and {0001} slip are responsible for the formation of strong {0002} basal texture and thus, poor ductility of Mg alloys restricting the widespread use of these alloys in aircraft and automotive industries. In the current research, for the first time, we use the ⟨0001⟩||RD as an initial texture for suppression of basal slip and the continuous β-$Mg_{17}Al_{12}$ phase for inhibition of extension twinning, simultaneously, to obtain non-basal orientations in the asymmetrically cold-rolled AZ91 magnesium alloy. The behavior of the Mg–9Al–1Zn alloy under asymmetric cold rolling is discussed based on the microstructural characterization and texture evolution.

Materials and Methods

The starting material was an experimental AZ91 (Mg–8.4Al–1.3Zn–0.3Mn) cast ingot. A quantometer device (Hitachi High-Tech Foundry-Master Smart) was employed to specify the chemical composition of the starting material. Sheets with dimensions of 70 × 20 × 3.5 mm were cut from the as-cast alloy. To prevent the formation of extension twins (which encourage basal texture), first, the as-cast microstructure was used without homogenization heat treatment. Second, with the preliminary analysis that was done on the texture of the as-cast ingot, it was tried that when cutting the casting sample and turning it into a sheet for the rolling process, the ⟨0001⟩ directions of most of the grains should be parallel to the direction in which the rolling is to be performed.

The asymmetric cold rolling with thickness reductions of 8 and 15% were performed at room temperature without lubricant by the single-roll drive rolling method. The rotational speed of the drive (down) roller was 2 rpm, and the diameter of both rollers was 150 mm. The thickness reduction per rolling pass was about 3%. Microstructural observations were carried out on the RD-TD section. The samples were mechanically ground with SiC papers, polished, and etched by the Picral reagent (4.26 g picric acid, 10 ml acetic acid, 10 ml distilled H_2O, and 150 ml ethanol). Textures of samples were conducted using X-ray diffraction (XRD, PANalytical, Cu Kα). Incomplete pole figures (PFs) were analyzed by TexTools software.

Results and Discussion

The micrographs of as-cast and deformed samples are shown in Figure 1. The boundaries (both grain and twin boundaries) can be classified by different neighbor misorientations: low (0°–15°), high (15°–65°), and extra high (65°–100°) angle boundaries (LABs, HABs, and EHABs, respectively). The relationship between the fraction of three different boundaries and the rolling reduction is depicted in Figure 2. The as-cast micrograph consisted of α + β eutectic and α-Mg with two intermetallic phases: $Mg_{17}Al_{12}$ and Al_8Mn_5. Intermetallic compounds are located at the boundaries of α and inside the grains. From Figure 1a, no twins are observed in the as-cast sample. The fractions of LABs, HABs, and EHABs for the as-cast sample are 1.6, 51.7, and 46.6%, respectively (see Fig. 2). After 8% asymmetric cold rolling (Figure 1b), several twins are observed in the microstructure. Contraction twins have thin and extended morphology, while extension twins have thick and lenticular morphology [35–41]. Therefore, a lot of $\left\{10\overline{1}1\right\}$ contraction twins (red arrows) and a few $\{10\overline{1}2\}$ extension twins (blue arrows) were created in the 8% rolled sample. Twins in Mg alloys have an angle with respect to the basal plane: 86° for the $\{10\overline{1}2\}$ extension twin formed owing to the extension of the *c*-axis, 56° for the $\{10\overline{1}1\}$ contraction twin developed by the compression of the *c*-axis, and 38° for the $\{10\overline{1}1\} - \{10\overline{1}2\}$ double twin [3, 4, 6–8, 12, 14, 16, 23–27, 30, 31, 36]. Figure 2 indicates that by 8% deformation, the fraction of HABs is increased which is mainly owing to the creation of many compression and/or double twins. The distribution of twins in the microstructure of 8% cold rolled is not

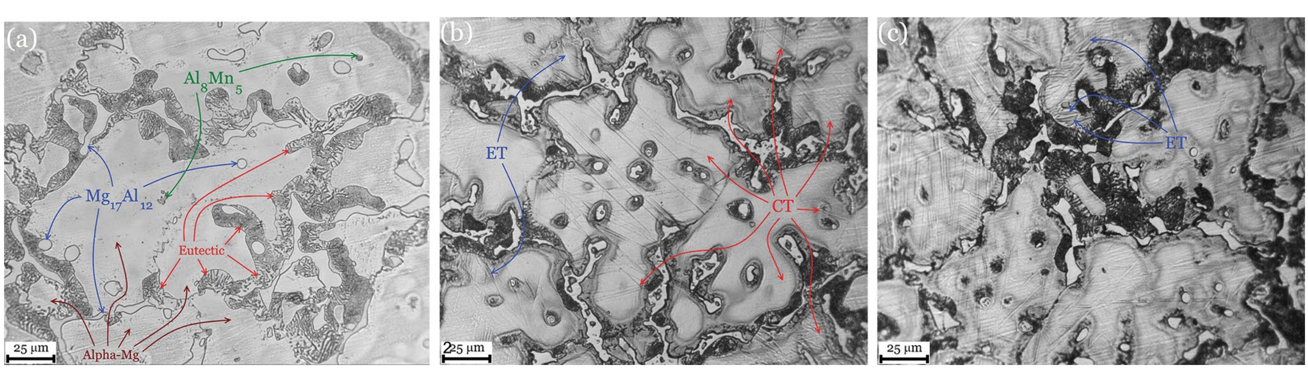

Fig. 1 The micrographs of (**a**) 0% (as-cast), (**b**) 8% rolled, and (**c**) 15% rolled samples

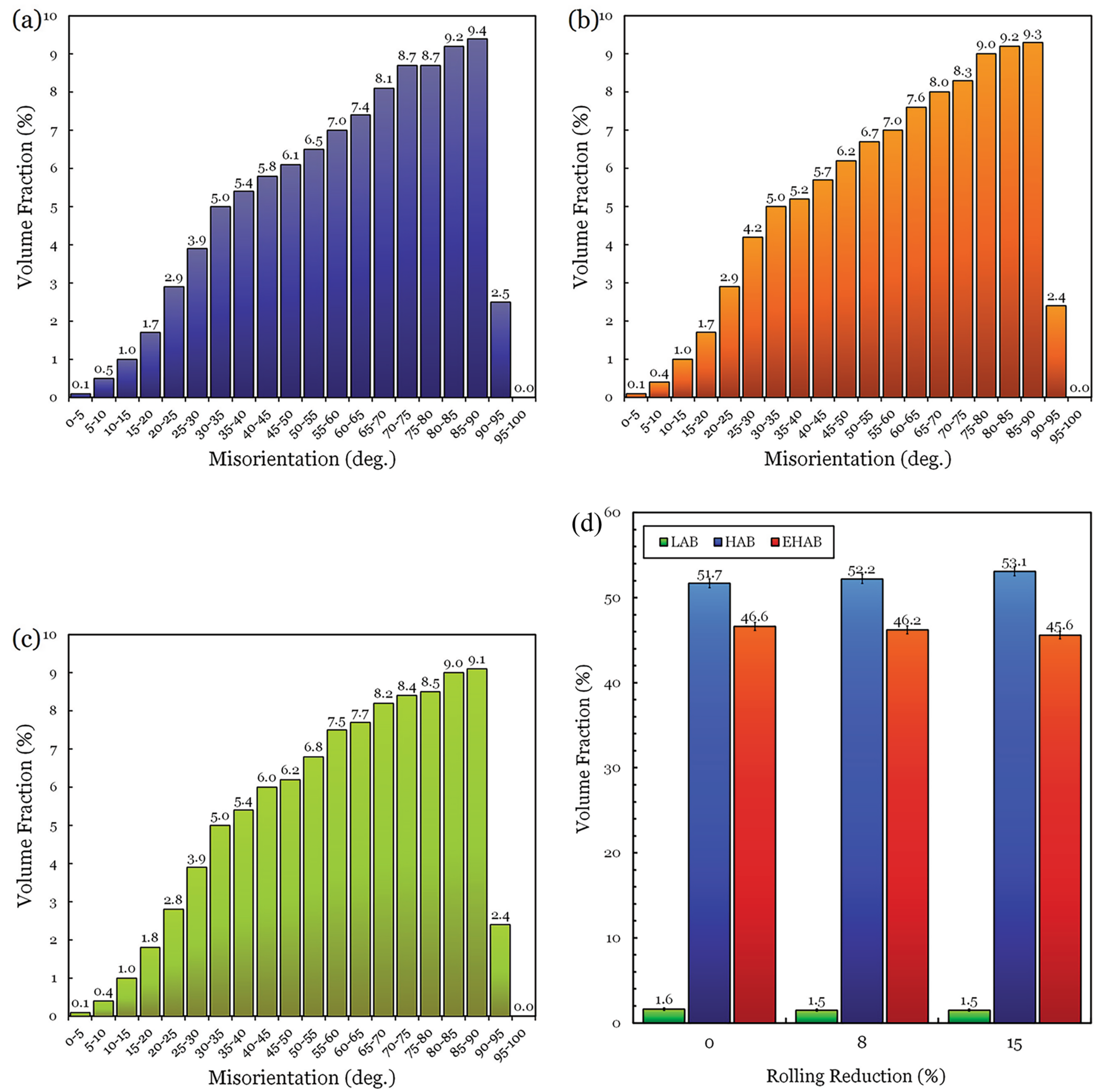

Fig. 2 The distributions of misorientation of (**a**) 0% (as-cast), (**b**) 8% rolled, and (**c**) 15% rolled samples, and (**d**) the volume fraction of LAB, HAB, and EHAB for different samples

homogeneous. In fact, the fraction of twins in the different grains is not equal and there are some twin-free grains. This is owing to the different initial orientations of grains. From Figure 1c, with increasing the deformation up to 15%, the number of contraction twins greatly increased, while there are some extension twins in the microstructure of AZ91. These results are confirmed in Figure 2. The distribution of twins becomes homogeneous, and all grains have many twins.

The PFs and orientation distribution functions (ODFs) of undeformed and deformed samples are demonstrated in Figures 3 and 4, respectively. In addition, Figure 5 depicts the fraction of the important texture orientations for samples with rolling deformation of 0, 8, and 15%. As seen, the starting alloy exhibits a ⟨0001⟩||RD fiber texture which means {0001} of most grains are parallel to the TD–ND surface. From Figures 4 and 5, the main

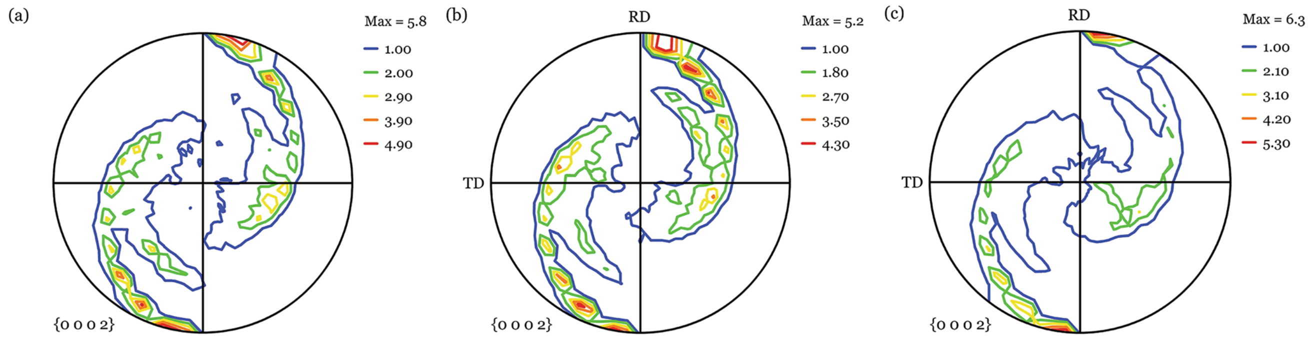

Fig. 3 The PFs of (**a**) 0% (as-cast), (**b**) 8% rolled, and (**c**) 15% rolled samples

orientations of the as-cast alloy are $\{10\bar{1}0\}\langle11\bar{2}6\rangle$, $\{10\bar{1}0\}\langle0001\rangle$, $\{11\bar{2}3\}\langle1\bar{1}00\rangle$, $\{11\bar{2}2\}\langle1\bar{1}00\rangle$, and $\{10\bar{1}2\}\langle20\bar{2}1\rangle$ with the intensity of 116.6 × R, 62.3 × R, 16.9 × R, 5.7 × R, and 5.5 × R, respectively. The well-known texture of magnesium alloys, i.e., {0002} basal texture, is absent. After an 8% thickness reduction, the overall texture intensity is decreased (see Figures 3 and 4). The strongest component is $\{10\bar{1}0\}\langle0001\rangle$ texture with an intensity of 43.4 × R. The other components are $\{11\bar{2}3\}\langle1\bar{1}00\rangle$, $\{10\bar{1}0\}\langle11\bar{2}6\rangle$, $\{10\bar{1}2\}\langle20\bar{2}1\rangle$, and $\{11\bar{2}2\}\langle1\bar{1}00\rangle$ with the intensity of 18.6 × R, 7.6 × R, 3.3 × R, and 2.9 × R, respectively. Moreover, the intensity of $\{0001\}\langle4\bar{5}10\rangle$ as a basal texture component increased from 0.5 × R to 0.9 × R. With an increase in the strain up to 15%, the intensity of $\{11\bar{2}3\}\langle1\bar{1}00\rangle$, $\{10\bar{1}2\}\langle20\bar{2}1\rangle$, and $\{11\bar{2}2\}\langle1\bar{1}00\rangle$ remains almost unchanged. On the other hand, the intensity of $\{10\bar{1}0\}\langle0001\rangle$, $\{10\bar{1}0\}\langle11\bar{2}6\rangle$, and $\{0001\}\langle4\bar{5}10\rangle$ significantly increased to 104.1 × R, 19.6 × R, and 5.5 × R, respectively. Therefore, the overall texture intensity increased. As also suggested in Figure 3c, there is no sign of basal fiber texture. This is an interesting result. From the results obtained from previous studies in Refs. [4, 10, 14, 19, 21, 22, 26, 29, 31, 32, 35], it is reported that the {0002} texture becomes very strong even at very low rolling reductions due to slip and twinning mechanisms. The present work indicated that achieving non-basal texture in magnesium alloys during rolling deformation is possible. Two important reasons can explain these results:

On the one hand, achieving a non-basal texture is related to the primary intense ⟨0001⟩||RD orientation, which is not favored for prismatic and basal slips. The strong ⟨0001⟩||RD orientation increases the activity of the pyramidal $\langle c+a\rangle$ slip system during cold deformation owing to its high Schmid factor. However, the pyramidal $\langle c+a\rangle$ slip cannot be activated at low deformation temperature due to its high CRSS. Therefore, it can be concluded that the primary intense ⟨0001⟩||RD orientation inhibits the slip mechanism during cold deformation. Consequently, the initial ⟨0001⟩||RD texture decreases the contribution of {0001} slip during deformation and weakens the basal orientation.

On the other hand, the extension twins have a great impact on the orientation development and formation of {0002} basal texture, because the {0001} of the twinned alpha-Mg grains are tilted by 86° from their original orientations (due to the extension twinning) and the orientation of the as-cast sample (i.e., ⟨0001⟩||RD) rotates to ⟨0001⟩||ND (or basal texture). In contrast, the contribution of double and contraction twins for the formation of {0001} texture is low. Double and contraction twins have an orientation relationship of 38° and 56° rotations between the untwined matrix and the twin variants [25, 28, 33]. However, the CRSS of extension twinning is much smaller than that of contraction or double ones [30, 34, 35], and the strong ⟨0001⟩||RD texture is also favored for extension twinning. Therefore, the activation of contraction twinning in AZ91 alloy is very difficult. Surprisingly, Figure 1 indicates that contraction twinning is the main deformation mode during cold rolling. This result is due to the β-$Mg_{17}Al_{12}$ located at the boundaries of alpha grains which can significantly limit the nucleation of thick extension twins. Beyerlein and coworkers [42] stated that the nucleation of twins can depend on the misorientation of the grain boundaries. The extension twins connected to grain boundary with smaller misorientations (< 45°) are more than those with larger misorientations. In fact, by enhancing the coherency of the boundary, the chance of the nucleation of the extension twin increases. Thus, it can be said that the incoherent $Mg_{17}Al_{12}$ located at the boundaries can hinder the nucleation of thick extension twins, but not suppress the nucleation of narrow double and contraction twins. Also, the extension twins usually nucleate at the boundary followed by

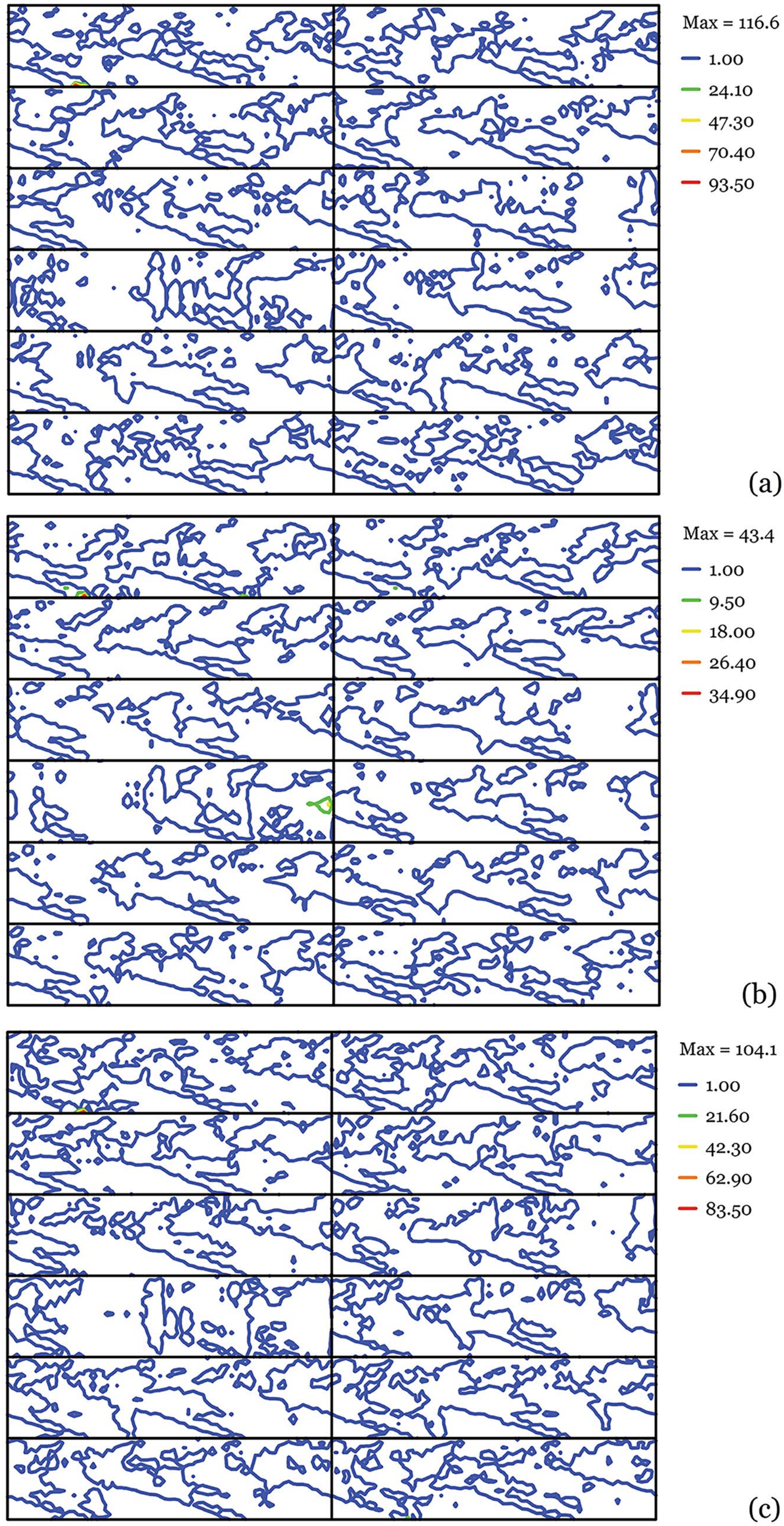

Fig. 4 The ODFs of (**a**) 0% (as-cast), (**b**) 8% rolled, and (**c**) 15% rolled samples

Fig. 5 Peak intensity of main orientations as a function of rolling deformation

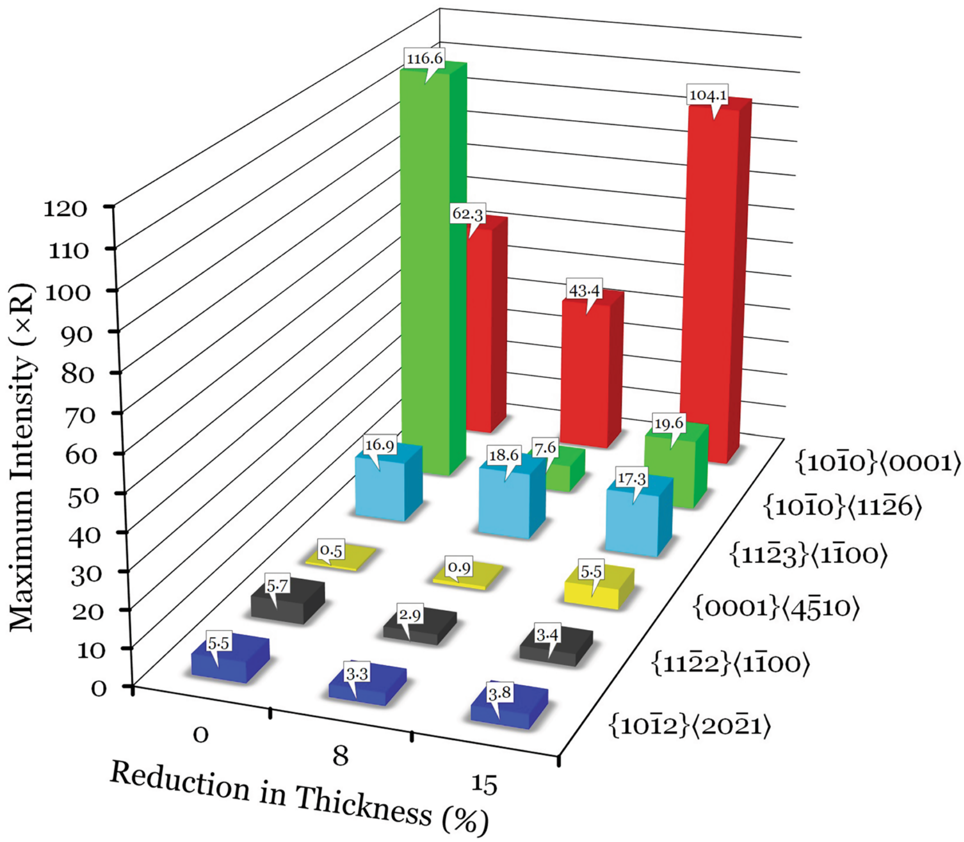

a rapid propagation within the alpha-Mg grain and finishing at the next boundary. The finishing of the extension twins at a boundary will create a localized stress concentration which would stimulate and trigger the nucleation of the twin in the next alpha-Mg grain [43, 44]. The high content of the continuous $Mg_{17}Al_{12}$ phase can suppress the nucleation of thick extension twins in the neighboring alpha-Mg grain.

Conclusions

In the present work, we used the ⟨0001⟩||RD as an initial texture for suppression of basal slip and the continuous β-$Mg_{17}Al_{12}$ phase for inhibition of extension twinning, simultaneously, to obtain non-basal orientation in the AZ91 magnesium alloy processed by asymmetric cold rolling. The as-cast sample consisted of α + β eutectic and α-Mg with two intermetallic phases, i.e., $Mg_{17}Al_{12}$ and Al_8Mn_5 which were located along grain boundaries and also inside the grains. By 8% and 15% rolling reductions, the fraction of HABs increased which was mainly owing to the formation of many contraction and/or double twins. Achieving non-basal texture was firstly due to the initial intense ⟨0001⟩||RD orientation, which was not favored for prismatic and basal slips. Also, the pyramidal slip could not be activated at low deformation temperatures due to its high CRSS. Secondly, the incoherent $Mg_{17}Al_{12}$ located at the boundaries of alpha-Mg suppressed the thick extension twin nucleation but did not inhibit the nucleation of narrow double and contraction twins.

References

1. I.J. Polmear, Magnesium alloys and applications. Mater. Sci. Technol. **10**, 1–16 (1994)
2. J. Singh, M.S. Kim, S.H. Choi, The effect of initial texture on micromechanical deformation behaviors in Mg alloys under a mini-V-bending test. Int. J. Plast. **117**, 33–57 (2019)
3. T. Krajňák, P. Minárik, J. Gubicza, K. Máthis, R. Kužel, M. Janeček, Influence of equal channel angular pressing routes on texture, microstructure and mechanical properties of extruded AX41 magnesium alloy. Mater Charact. **123**, 282–293 (2017)
4. A. Imandoust, C.D. Barrett, A.L. Oppedal, W.R. Whittington, Y. Paudel, H. El Kadiri, Nucleation and preferential growth mechanism of recrystallization texture in high purity binary magnesium-rare earth alloys. Acta Mater. **138**, 27–41 (2017)
5. X. Huang, K. Suzuki, Y. Chino, Influences of initial texture on microstructure and stretch formability of Mg–3Al–1Zn alloy sheet obtained by a combination of high temperature and subsequent warm rolling. Scripta Mater. **63**, 395–398 (2010)
6. N. Li, G. Huang, R. Xin, Q. Liu, Effect of initial texture on dynamic recrystallization and deformation mechanisms in AZ31 Mg alloy extruded at 573 K. Mater. Sci. Eng. A. **569**, 18–26 (2013)
7. Z. Yu, A. Tang, J. He, Z. Gao, J. She, J. Liu, F. Pan, Effect of high content of manganese on microstructure, texture and

mechanical properties of magnesium alloy. Mater Charact. **136**, 310–317 (2018)
8. L. Sun, J. Bai, F. Xue, L. Tao, C. Chu, J. Meng, Exceptional texture evolution induced by multi-pass cold drawing of magnesium alloy. Mater. Des. **135**, 267–274 (2017)
9. X. Huang, K. Suzuki, Y. Chino, M. Mabuchi, Influence of initial texture on cold deep drawability of Mg–3Al–1Zn alloy sheets. Mater. Sci. Eng. A. **565**, 359–372 (2013)
10. D.C. Foley, M. Al-Maharbi, K.T. Hartwig, I. Karaman, L.J. Kecskesc, S.N. Mathaudhu, Grain refinement versus crystallographic texture: mechanical anisotropy in a magnesium alloy. Scripta Mater. **64**, 193–196 (2011)
11. H. Zhang, G. Huang, D. Kong, G. Sang, B. Song, Influence of initial texture on formability of AZ31B magnesium alloy sheets at different temperatures. J. Mater. Process. Technol. **211**, 1575–1580 (2011)
12. D. Guan, W. Mark Rainforth, L. Ma, B. Wynne, J. Gao, Twin recrystallization mechanisms and exceptional contribution to texture evolution during annealing in a magnesium alloy. Acta Mater. **126**, 132–144 (2017)
13. D. Sarker, J. Friedman, D.L. Chen, Twin growth and texture evolution in an extruded AM30 magnesium alloy during compression. J. Mater. Sci. Technol. **30**, 884–887 (2014)
14. Z.R. Zeng, Y.M. Zhu, S.W. Xu, M.Z. Bian, C.H.J. Davies, N. Birbilis, J.F. Nie, Texture evolution during static recrystallization of cold-rolled magnesium alloys. Acta Mater. **105**, 479–494 (2016)
15. Q. Yang, B. Jiang, Y. Tian, W. Liu, F. Pan, A tilted weak texture processed by an asymmetric extrusion for magnesium alloy sheets. Mater. Lett. **100**, 29–31 (2013)
16. S. Biswas, S. Suwas, R. Sikand, A.K. Gupta, Analysis of texture evolution in pure magnesium and the magnesium alloy AM30 during rod and tube extrusion. Mater. Sci. Eng. A. **528**, 3722–3729 (2011)
17. T. Krajňák, P. Minárik, J. Stráská, J. Gubicza, K. Máthis, M. Janeček, Influence of equal channel angular pressing temperature on texture, microstructure and mechanical properties of extruded AX41 magnesium. J. Alloy. Compd. **705**, 273–282 (2017)
18. Z. Zhang, The formation of double peaks in the basal texture during ambient extrusion of an AZ31 magnesium alloy. Mater. Lett. **116**, 131–134 (2014)
19. T. Al-Samman, X. Li, Sheet texture modification in magnesium-based alloys by selective rare earth alloying. Mater. Sci. Eng. A. **528**, 3809–3822 (2011)
20. A. Hadadzadeh, M.A. Wells, S. Kumar Shaha, H. Jahed, B.W. Williams, Role of compression direction on recrystallization behavior and texture evolution during hot deformation of extruded ZK60 magnesium alloy. J. Alloys Compd. **702**, 274–289 (2017)
21. D.G. Kim, K.M. Lee, J.S. Lee, Y.O. Yoon, H.T. Son, Evolution of microstructures and textures in magnesium AZ31 alloys deformed by normal and cross-roll rolling. Mater. Lett. **75**, 122–125 (2012)
22. Z. Sun, Y. Wu, Y. Xin, Y. Peng, B. Feng, Q. Liu, Varying the strong basal texture in a Mg–3Al–1Zn plate by a new wave-shaped interface rolling. Mater. Lett. **213**, 151–153 (2018)
23. L. Wang, E. Mostaed, X. Cao, G. Huang, A. Fabrizi, F. Bonollo, C. Chi, M. Vedani, Effects of texture and grain size on mechanical properties of AZ80 magnesium alloys at lower temperatures. Mater. Des. **89**, 1–8 (2016)
24. M.R. Barnett, A. Sullivan, N. Stanford, N. Ross, A. Beer, Texture selection mechanisms in uniaxially extruded magnesium alloys. Scripta Mater. **63**, 721–724 (2010)
25. L. Song, B. Wu, L. Zhang, X. Du, Y. Wang, C. Esling, Twinning characterization of fiber-textured AZ31B magnesium alloy during tensile deformation. Mater. Sci. Eng. A. **710**, 57–65 (2018)
26. S.H. Park, S. Hong, S.C. Lee, In-plane anisotropic deformation behavior of rolled Mg–3Al–1Zn alloy by initial 10–12 twins. Mater. Sci. Eng. A. **570**, 149–163 (2013)
27. O. Muránsky, M.R. Barnett, D.G. Carr, S.C. Vogel, E.C. Oliver, Investigation of deformation twinning in a fine-grained and coarse-grained ZM20 Mg alloy: combined in situ neutron diffraction and acoustic emission. Acta Mater. **58**, 1503–1517 (2010)
28. K. Yoshida, Prediction of ductile fracture induced by contraction twinning in AZ31 sheet subjected to uniaxial and biaxial stretching modes. Int. J. Plast. **84**, 102–137 (2015)
29. X. Huang, K. Suzuki, Y. Chino, M. Mabuchi, Influence of rolling temperature on static recrystallization behavior of AZ31 magnesium alloy. J. Mater. Sci. **47**, 4561–4567 (2012)
30. D. Hou, T. Liu, L. Luo, L. Lu, H. Chen, D. Shi, Twinning behaviors of a rolled AZ31 magnesium alloy under multidirectional loading. Mater Charact. **124**, 122–128 (2017)
31. Y. Xin, M. Wang, Z. Zeng, G. Huang, Q. Liu, Tailoring the texture of magnesium alloy by twinning deformation to improve the rolling capability. Scripta Mater. **64**, 986–989 (2011)
32. J. Luo, W.W. Hu, Q.Q. Jin, H. Yan, R.S. Chen, Unusual cold rolled texture in an Mg–2.0Zn–0.8Gd sheet. Scripta Mater. **127**, 146–150 (2017)
33. A. Levinson, R.K. Mishra, R.D. Doherty, S.R. Kalidindi, Influence of deformation twinning on static annealing of AZ31 Mg alloy. Acta Mater. **61**, 5966–5978 (2013)
34. P. Yang, Y. Yu, L. Chen, W. Mao, Experimental determination and theoretical prediction of twin orientations in magnesium alloy AZ31. Scripta Mater. **50**, 1163–1168 (2014)
35. J. Koike, Enhanced deformation mechanisms by anisotropic plasticity in polycrystalline Mg alloys at room temperature. Metall. Mater. Trans. A. **36**, 1689–1696 (2005)
36. D. Sarker, J. Friedman, D.L. Chen, De-twinning and texture change in an extruded AM30 magnesium alloy during compression along normal direction. J. Mater. Sci. Technol. **31**, 264–268 (2015)
37. H.A. Patel, D.L. Chen, S.D. Bhole, K. Sadayappan, Low cycle fatigue behavior of a semi-solid processed AM60B magnesium alloy. Mater. Des. **49**, 456–464 (2013)
38. Y. Zhang, D. Kent, G. Wang, D. StJohn, M.S. Dargusch, The cold-rolling behaviour of AZ31 tubes for fabrication of biodegradable stents. J. Mech. Behav. Biomed. Mater. **39**, 292–303 (2014)
39. M. Kavyani, G.R. Ebrahimi, M. Sanjari, M. Haghshenas, Texture evaluation in warm deformation of an extruded Mg–6Al–3Zn alloy. J. Magn. Alloys. **4**, 89–98 (2016)
40. L. Lu, J. Zhao, L. Liu, G. Wang, Microstructural study of cold forged and annealed Mg alloys. Mater. Sci. Technol. **32**, 104–110 (2016)
41. F. Mokdad, D.L. Chen, D.Y. Li, Single and double twin nucleation, growth, and interaction in an extruded magnesium alloy. Mater. Des. **119**, 376–396 (2017)
42. I.J. Beyerlein, L. Capolungo, P.E. Marshall, R.J. McCabe, C.N. Tome, Statistical analyses of deformation twinning in magnesium. Phil. Mag. **90**, 2161–2190 (2010)
43. J.J. Jonas, S. Mu, T. Al-Samman, G. Gottstein, L. Jiang, E. Martin, The role of strain accommodation during the variant selection of primary twins in magnesium. Acta Mater. **59**, 2046–2056 (2011)
44. S. Niknejad, S. Esmaeili, N.Y. Zhou, The role of double twinning on transgranular fracture in magnesium AZ61 in a localized stress field. Acta Mater. **102**, 1–16 (2016)